

Excluded-Volume Effects on the Mean-Square Radius of Gyration of Oligo- and Polystyrenes in Dilute Solutions

Fumiaki Abe, Yoshiyuki Einaga, Takenao Yoshizaki, and Hiromi Yamakawa*

Department of Polymer Chemistry, Kyoto University, Kyoto 606-01, Japan

Received November 16, 1992; Revised Manuscript Received January 12, 1993

ABSTRACT: The mean-square radius of gyration $\langle S^2 \rangle$ was determined by small-angle X-ray scattering and light scattering for atactic oligo- and polystyrenes (a-PS) in toluene at 15.0 °C in the range of weight-average molecular weight M_w from 5.78×10^2 to 3.84×10^6 . The solvent and temperature have been chosen so that the unperturbed dimension $\langle S^2 \rangle_0$ of the a-PS chain in that good solvent may coincide with that in cyclohexane at 34.5 °C (Θ) taken as a reference standard. The radius expansion factor α_S determined from $\langle S^2 \rangle$ and $\langle S^2 \rangle_0$ decreases extremely rapidly for small M_w with decreasing M_w and tends to unity at finite M_w , in contrast to the two-parameter theory prediction. The implication is that there are significant effects of chain stiffness on α_S . The results may be quantitatively explained by the Yamakawa-Stockmayer-Shimada theory based on the wormlike and helical wormlike (HW) chain models, with an appropriate value of the excluded-volume strength B along with those of the HW model parameters established from dilute solution properties of a-PS in the unperturbed state. The theory predicts that the effect of chain stiffness on α_S remains rather large even at very large $M_w \sim 10^6$ for a-PS. It is also shown that the recent renormalization group theory of α_S by Chen and Noolandi does not work well, yielding a large discrepancy from the present experimental results.

Introduction

The excluded-volume effect has long been a central problem of polymer solution theory and was already given prominence in Flory's 1953 book.¹ A number of theoretical investigations of the problem performed before about 1970 are systematically summarized as the so-called two-parameter theory in the book by Yamakawa² with a comparison with extensive experimental data. This first stage of research was immediately followed by a new theoretical approach, namely, the renormalization group theory. Its developments made until recently are found in books by Freed³ and by des Cloizeaux and Jannink,⁴ and it still continues at the present time. However, for flexible polymers it is still essentially a two-parameter theory. More important is the fact that during the past 2 decades, there have been many experimental findings that indicate the breakdown of the two-parameter theory, as summarized and discussed very recently by Fujita in his 1990 book.⁵

Among them, most remarkable is the finding that for flexible polymers in good solvents the interpenetration function Ψ appearing in the second virial coefficient A_2 decreases with increasing molecular weight M before reaching its constant limiting value.⁶ Very recently, Yamakawa⁷ has emphasized that this is due to the fact that the effect of chain stiffness remains rather large even for such large M that the ratio of the unperturbed mean-square radius of gyration $\langle S^2 \rangle_0$ to M already reaches its coil limiting value independent of M . His analysis is based on a generalization of the Yamakawa-Stockmayer (YS) theory⁸ of A_2 for the Kratky-Porod (KP) wormlike chain⁹ to the helical wormlike (HW) chain,^{10,11} in conjunction with the corresponding generalization of the YS theory⁸ of the expansion factor α_S for (perturbed) $\langle S^2 \rangle$ by Yamakawa and Shimada.^{12,13} This Yamakawa-Stockmayer-Shimada (YSS) theory predicts that the chain stiffness has a significant effect also on α_S even for large M mentioned above. Indeed, the reanalysis of Ψ above was motivated by this prediction.

Thus the main purpose of the present and forthcoming papers is to confirm experimentally these predictions. In the present paper, we make a study of α_S for atactic

polystyrene (a-PS). We note that a similar experimental study has already been made by Huber et al.¹⁴ for the same system and also by Kitagawa et al.¹⁵ for poly-(isophthaloyl-*trans*-2,5-dimethylpiperazine) in *N*-methyl-2-pyrrolidone, comparing the results with the YS or YSS theory, but that they have not directly determined the unperturbed values $\langle S^2 \rangle_0$ that are required to estimate α_S .

In order to examine the validity of the HW chain model itself in the unperturbed Θ state, in a series of recent experimental work¹⁶ we have measured systematically equilibrium conformational and steady-state transport properties for various flexible polymers over a wide range of M , including the oligomer region, with a determination of their model parameters. In particular, we have already determined $\langle S^2 \rangle_0$ for a-PS in cyclohexane at 34.5 °C (Θ) from small-angle X-ray scattering (SAXS) and light scattering (LS) measurements, using well-characterized samples of narrow molecular weight distribution and fixed stereochemical composition (the fraction of racemic diads $f_r = 0.59$).¹⁷ In the present work, a similar determination is made of $\langle S^2 \rangle$ for a-PS in a good solvent, toluene, at 15.0 °C, using the same samples as above.

Now there arises the question of whether the value of α_S in a given good solvent at a given temperature may be or may not be calculated from $\alpha_S^2 = \langle S^2 \rangle / \langle S^2 \rangle_0$ with the value of $\langle S^2 \rangle$ in that solvent at that temperature and with the value of $\langle S^2 \rangle_0$ in an appropriate Θ solvent at the Θ temperature different from the given temperature. This usual procedure is of course valid if the unperturbed chain dimension $\langle S^2 \rangle_0$ is independent of solvent and temperature. However, this is not generally the case, as has been long recognized.^{18,19} Rigorously, we must then adopt as $\langle S^2 \rangle_0$ the unperturbed value that $\langle S^2 \rangle$ would have if the excluded-volume interaction were absent in the given good solvent at the given temperature. In fact, such an unperturbed state may be realized in the oligomer region without intramolecular excluded-volume interaction even in a good solvent. Thus, for convenience, in the present work we adopt as $\langle S^2 \rangle_0$ the value in cyclohexane at 34.5 °C and determine a temperature at which $\langle S^2 \rangle$ is to be measured so that the value of $\langle S^2 \rangle$ may be identical with

Table I
Values of M_w , x_w , and M_w/M_n for Atactic Oligo- and Polystyrenes

sample	M_w	x_w	M_w/M_n
OS5 ^a	5.78×10^2	5	1.00
OS6	6.80×10^2	5.98	1.00
OS8	9.04×10^2	8.13	1.01
A1000-b ^b	1.48×10^3	13.7	1.02
A2500-a'	1.78×10^3	16.6	1.04
A2500-a	2.27×10^3	21.3	1.05
A2500-b	3.48×10^3	32.9	1.07
A5000-3	5.38×10^3	51.2	1.03
F1-2	1.01×10^4	96.6	1.03
F2 ^c	2.05×10^4	197	1.02
F4	4.00×10^4	384	1.02
F10	9.73×10^4	935	1.02
F20	(1.91×10^5)	1840	1.02
F40	3.59×10^5 (3.57×10^5)	3450	1.01
F80	7.32×10^5 (7.23×10^5)	7040	1.01
F128-2	1.32×10^6 (1.29×10^6)	12700	1.05
F288-a	3.52×10^6	33800	1.03
F380 ^d	3.84×10^6 (3.94×10^6)	36900	1.05

^a M_w 's of OS5 through OS8 had been determined from GPC.¹⁶

^b M_w 's of A1000-b through F1-2 had been determined from LS in methyl ethyl ketone at 25.0 °C.^{16,20} ^c M_w 's of F2 through F288-a had been determined from LS in cyclohexane at 34.5 °C,^{17,21} the figures in parentheses representing the values in toluene at 15.0 °C (present work). ^d M_w 's were determined from LS in cyclohexane at 34.5 °C and in toluene at 15.0 °C (the value in parentheses) in this work.

that of $\langle S^2 \rangle_0$ in the oligomer region, choosing a suitable good solvent. In practice, we have preliminarily done this using values of the intrinsic viscosity $[\eta]$ of the styrene oligomers in cyclohexane at 34.5 °C and in a good solvent. The good solvent thus chosen is toluene, and the temperature determined for that solution is 15.0 °C.

Experimental Section

Materials. Most of the a-PS samples used in this work are the same as those used in the previous studies of the mean-square optical anisotropy $\langle \Gamma^2 \rangle$,¹⁶ $[\eta]$,²⁰ $\langle S^2 \rangle_0$,¹⁷ the transport factors ρ and Φ for long flexible chains,²¹ and the translational diffusion coefficient D ,²² i.e., the fractions separated from the standard samples supplied by Tosoh Co., Ltd., by preparative gel permeation chromatography (GPC) or fractional precipitation. The additional samples F20 and F380 used in this work are also the standard samples of Tosoh Co., Ltd. All the samples have a fixed stereochemical composition of $f_r = 0.59$ independent of molecular weight. The values of the weight-average molecular weight M_w , the weight-average degree of polymerization x_w , and the ratio of M_w to the number-average molecular weight M_n are listed in Table I. It also includes the values of M_w determined from the present LS measurements for the samples F20, F40, F80, F128-2, and F380 in toluene at 15.0 °C and for F380 in cyclohexane at 34.5 °C. It is seen that the values of M_w determined for the same sample in the different solvents are in good agreement with each other. As seen from the values of M_w/M_n , all the samples are sufficiently narrow in molecular weight distribution.

The solvent toluene was purified by distillation after refluxing over sodium for ca. 6 h, prior to use.

Viscosity. Viscosity measurements were carried out for six oligostyrene samples with M_w ranging from 578 (pentamer) to 2270 in order to choose a suitable good solvent and determine a temperature at which $\langle S^2 \rangle$ is to be measured in that solvent, as mentioned in the Introduction. In this preliminary experiment, $[\eta]$ were determined in toluene at 15.0 and 25.0 °C. We used spiral capillary viscometers of the Ubbelohde type to have long flow times of the test solutions and solvent so that the relative and specific viscosities might be determined with sufficient accuracy. Density corrections were made in the calculation of the relative viscosity from the flow times of the solution and solvent.

The test solutions were prepared gravimetrically and their polymer mass concentrations c (in g/cm³) were calculated from

their weight fractions by using the densities of the respective solutions measured with a pycnometer of the Lipkin-Davison type.

Small-Angle X-ray Scattering. SAXS measurements were carried out for the 11 a-PS samples with $M_w \leq 4.00 \times 10^4$ in toluene at 15.0 °C by using an Anton Paar Kratky U-slit camera with an incident X-ray of wavelength 1.54 Å (Cu K α line). The apparatus system and the methods of data acquisition and analysis are the same as those described in the previous paper.¹⁷

The measurements were performed for 4–7 solutions of different concentrations for each polymer sample and for the solvent at scattering angles ranging from 1×10^{-3} rad to a value at which the scattering intensity was negligibly small. Corrections for the stability of the X-ray source and the detector electronics were made by measuring the intensity scattered from Lupolene (a platelet of polyethylene) used as a working standard before and after each measurement for a given sample solution and the solvent. The effect of absorption of X-ray by a given solution or solvent was also corrected by measuring the intensity scattered from Lupolene with insertion of the solution or solvent between the X-ray source and Lupolene. The degree of absorption increased linearly with increasing solute concentration.

The excess reduced scattering intensities were obtained from the observed (smeared) excess reduced intensities by the modified Glatter desmearing method, which consists of expressing the true scattering function in terms of cubic B-spline functions, as described before.¹⁷ All the data were processed by the use of a Fujitsu M-1800/30 digital computer in this university. Then the desmeared excess reduced intensities were analyzed by using the Berry square-root plot²³ to evaluate the apparent mean-square radius of gyration $\langle S^2 \rangle_s$.¹⁷

The test solutions were prepared gravimetrically, and their polymer mass concentrations c were calculated from the weight fractions by using the densities of the respective solutions.

Light Scattering. LS measurements were carried out to obtain $\langle S^2 \rangle$ (and also M_w) for five a-PS samples with $M_w \geq 1.91 \times 10^5$ in toluene at 15.0 °C and for the sample F380 in cyclohexane at 34.5 °C (Θ). A Fica 50 light-scattering photometer was used for all the measurements with vertically polarized incident light of wavelength 436 nm. For a calibration of the apparatus, the intensity of light scattered from pure benzene was measured at 25.0 °C at a scattering angle of 90°, where the Rayleigh ratio $R_{90}(90^\circ)$ of pure benzene was taken as 46.5×10^{-6} cm⁻¹. The depolarization ratio ρ_u of pure benzene at 25.0 °C was determined to be 0.41 ± 0.01 . The scattering intensities were measured for solutions of five different concentrations for each polymer sample and for the solvent at scattering angles θ ranging from 30 to 150° except for the highest molecular weight sample F380 in toluene, for which θ was changed from 15 to 30°. The obtained data were analyzed by the Berry square-root plot as in the case of the SAXS measurements. Here, values of M_w and the second virial coefficient A_2 were determined for each sample, in addition to $\langle S^2 \rangle$. The present results for M_w are given in Table I.

The most concentrated solution of each sample in toluene was prepared gravimetrically and made homogeneous by continuous stirring for ca. 1 day at room temperatures. These solutions and solvent were made dust-free by filtration through a Teflon membrane of pore size 0.45 μ m. The solutions of lower concentrations were obtained by successive dilution. The polymer mass concentrations c were calculated from the weight fractions by using the densities of the solutions.

The value of the refractive index increment $\partial n/\partial c$ measured at 436 nm by the use of a Shimadzu differential refractometer was 0.110₈ cm³/g for a-PS in toluene at 15.0 °C.

Results

Intrinsic Viscosity of Atactic Oligostyrene. In Figure 1, the values (unfilled circles) of $[\eta]$ for the oligostyrene samples in toluene at 15.0 °C are compared with those (filled circles) of $[\eta]_\Theta$ determined previously²⁰ for the same samples in cyclohexane at 34.5 °C (Θ), in the range of M_w from 578 to 2270, for which the excluded-volume effect on $[\eta]$ may be neglected. It is seen that the values obtained under the two different solvent conditions

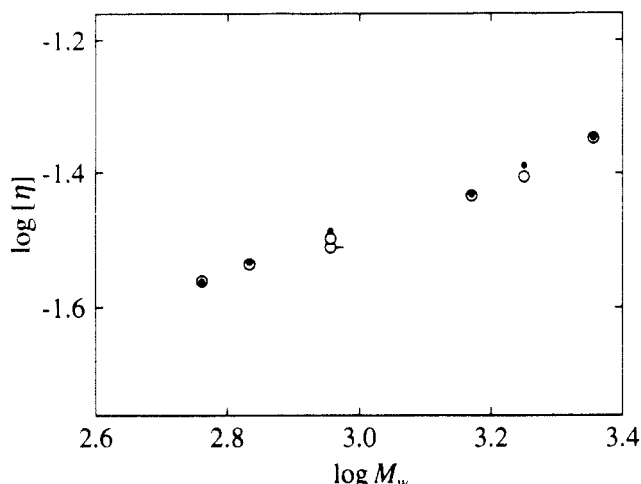


Figure 1. Double-logarithmic plots of $[\eta]$ (in dL/g) against M_w for oligostyrene: (O) in toluene at 15.0 °C; (O-) in toluene at 25.0 °C; (●) in cyclohexane at 34.5 °C (Θ).²⁰

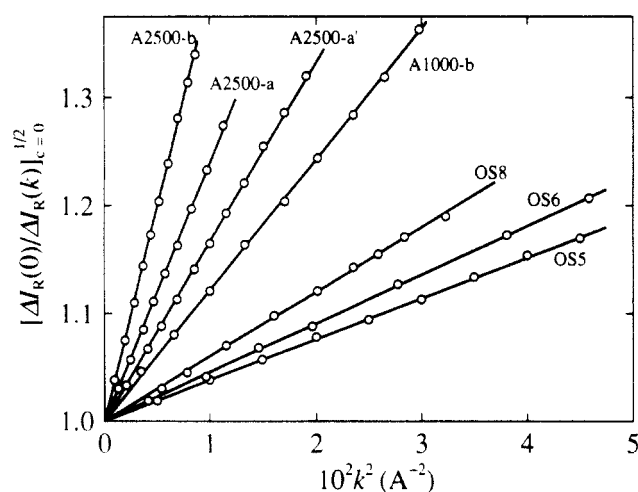


Figure 2. Plots of $[\Delta I_R(0)/\Delta I_R(k)]_{c=0}^{1/2}$ against k^2 for the indicated a-PS samples with $M_w \leq 3.48 \times 10^3$, obtained from SAXS in toluene at 15.0 °C.

are in good agreement with each other to within 1% except for the samples OS8 and A2500-a', for which the differences are somewhat larger, the values in toluene being 2.5 and 3.7% smaller for OS8 and A2500-a', respectively. The results indicate that the molecular dimensions of these oligomers may be considered the same under the two solvent conditions, provided that the hydrodynamic diameters of the a-PS chain in these solvents are the same (with the same Flory-Fox factor Φ). We note that this conclusion is confirmed by a direct determination of $\langle S^2 \rangle$ from SAXS measurements, as shown below. From Figure 1, it is also seen that the value (unfilled circle with pip) of $[\eta]$ for the sample OS8 in toluene at 25.0 °C is ca. 5% smaller than that of $[\eta]_0$, suggesting that the chain dimension at temperatures higher than 15.0 °C is appreciably different from that in cyclohexane at Θ . According to these findings, we have decided to use toluene at 15.0 °C as a good solvent for a-PS suitable for the present purpose.

Mean-Square Radii of Gyration $\langle S^2 \rangle_s$ and $\langle S^2 \rangle$. Figures 2 and 3 show plots of $[\Delta I_R(0)/\Delta I_R(k)]_{c=0}^{1/2}$, i.e., the inverse of the scattering function, against k^2 for all the samples examined by SAXS measurements in toluene at 15.0 °C, where $\Delta I_R(k)$ is the excess reduced scattering intensity and k is the magnitude of the scattering vector. The data points for each sample follow closely a straight line in the range of k displayed, thereby permitting an

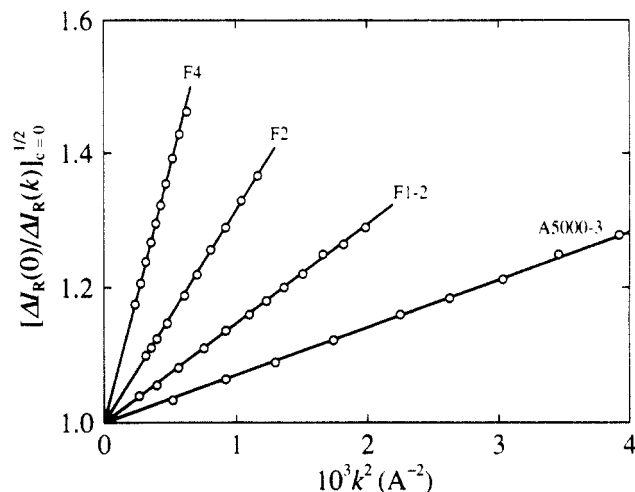


Figure 3. Plots of $[\Delta I_R(0)/\Delta I_R(k)]_{c=0}^{1/2}$ against k^2 for the indicated a-PS samples with $M_w \geq 5.38 \times 10^3$, obtained from SAXS in toluene at 15.0 °C.

Table II
Results of SAXS Measurements on Atactic Oligo- and Polystyrenes in Toluene at 15.0 °C and in Cyclohexane at 34.5 °C (Θ)

sample	toluene (15.0 °C)		cyclohexane (34.5 °C) ^a	
	$\langle S^2 \rangle_s^{1/2}$, Å	$\langle S^2 \rangle^{1/2}$, Å	$\langle S^2 \rangle_s^{1/2}$, Å	$\langle S^2 \rangle_0^{1/2}$, Å
OS5	4.79	3.45	4.75	3.39
OS6	5.20	4.00	5.14	3.92
OS8	5.98	4.98	5.89	4.87
A1000-b	8.52	7.85	8.66	7.99
A2500-a'	10.0	9.49	9.99	9.42
A2500-a	12.0	11.5	11.7	11.2
A2500-b	15.4	15.0	15.0	14.6
A5000-3	20.6	20.4	19.3	19.0
F1-2	29.5	29.3	27.5	27.3
F2	43.4	43.2	39.8	39.7
F4	66.9	66.9	56.7	56.6
F10			91.0	91.0

^a Reproduced from ref 17.

accurate determination of $\langle S^2 \rangle_s$ from its slope. The values of $\langle S^2 \rangle_s^{1/2}$ thus determined are listed in the second column of Table II.

As discussed previously,¹⁷ the values of $\langle S^2 \rangle_s$ contain contributions from the finite cross section of the polymer chain. Thus a correction must be made to draw $\langle S^2 \rangle$ of the chain contour from $\langle S^2 \rangle_s$, since for the former a theoretical expression has been derived to be compared with experiment. For this purpose, we may use the equation

$$\langle S^2 \rangle_s = \langle S^2 \rangle + S_c^2 \quad (1)$$

which has been derived for a continuous chain having a uniform circular cross section, with S_c being the radius of gyration of the cross section.¹⁷ In this work, we make the correction by adopting the value 11 Å² for S_c^2 estimated previously¹⁷ from the data for the partial specific volume v_2 of a-PS in cyclohexane at 34.5 °C. We note that the value of v_2 of a-PS in toluene at 15.0 °C is approximately equal to that in cyclohexane.

The results for $\langle S^2 \rangle^{1/2}$ thus obtained are given in the third column of Table II. It also includes the values of $\langle S^2 \rangle_s^{1/2}$ and $\langle S^2 \rangle_0^{1/2}$ obtained previously¹⁷ for the same a-PS samples in cyclohexane at 34.5 °C (Θ), for comparison. The value of $\langle S^2 \rangle^{1/2}$ or $\langle S^2 \rangle_0^{1/2}$ for the pentamer is seen to be ca. 30% smaller than that of $\langle S^2 \rangle_s^{1/2}$. The difference between them decreases progressively with increasing M_w and becomes negligible for $M_w > 2 \times 10^4$.

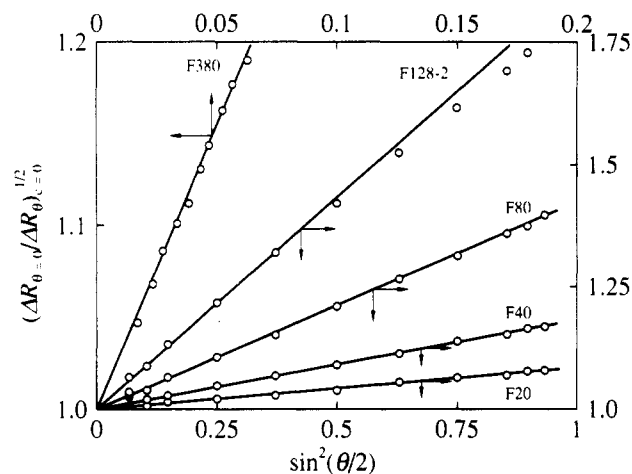


Figure 4. Plots of $(\Delta R_{\theta=0}/\Delta R_{\theta=0})^{1/2}$ against $\sin^2(\theta/2)$ for the indicated a-PS samples, obtained from LS in toluene at 15.0 °C.

Table III

Results of LS Measurements on Atactic Oligo- and Polystyrenes in Toluene at 15.0 °C and in Cyclohexane at 34.5 °C (Θ)

sample	toluene (15.0 °C) $\langle S^2 \rangle^{1/2}$, Å	cyclohexane (34.5 °C) ^a $\langle S^2 \rangle_0^{1/2}$, Å
F20	162	
F40	238	167
F80	363	240
F128-2	520	319
F288-a		521
F380	984	554

^a Reproduced from ref 21, except for the sample F380.

Figure 4 shows plots of $(\Delta R_{\theta=0}/\Delta R_{\theta=0})^{1/2}$ against $\sin^2(\theta/2)$ for all the samples examined by LS measurements in toluene at 15.0 °C, where ΔR_{θ} is the excess reduced intensity at a scattering angle θ . The data points for each sample at small θ are closely fitted by the straight line indicated, from whose slope the value of $\langle S^2 \rangle$ can be determined accurately. The results obtained for $\langle S^2 \rangle^{1/2}$ are summarized in Table III, along with the previous results²¹ for the same samples in cyclohexane at 34.5 °C (Θ).

Discussion

Dependence of $\langle S^2 \rangle/x_w$ on x_w . Figure 5 shows double-logarithmic plots of $[(\langle S^2 \rangle/x_w)/(\langle S^2 \rangle_0/x_w)]$ against x_w for the present results (unfilled circles) for a-PS in toluene at 15.0 °C along with those (filled circles) in cyclohexane at 34.5 °C (Θ). The solid curves connect the data points smoothly. Here, $(\langle S^2 \rangle_0/x_w)_\infty$ denotes the value of the ratio $\langle S^2 \rangle/x_w$ for the infinitely long unperturbed chain and was taken as 8.13 Å² from the average value of the LS data for the five highest-molecular-weight samples in cyclohexane at Θ . It should be noted that this value of $(\langle S^2 \rangle_0/x_w)_\infty$ is ca. 6% smaller than that by Miyaki et al.^{24,25} (The discrepancy may probably be due to the difference between the samples used in molecular weight distribution.²¹)

It is seen that, for $x_w < 20$, the values of $\langle S^2 \rangle/x_w$ in toluene at 15.0 °C are in good agreement with those of $\langle S^2 \rangle_0/x_w$ in cyclohexane at Θ , confirming the conclusion derived from the preliminary viscosity measurements shown in Figure 1. This agreement implies that the dimensions and conformations of the a-PS chain in the unperturbed state may be considered the same under the two solvent conditions. Thus this confirmation assures that we may calculate correctly the expansion factor α_S for a-PS in toluene at 15.0 °C by the use of the values of $\langle S^2 \rangle_0$ in cyclohexane at Θ as reference standards, i.e., by

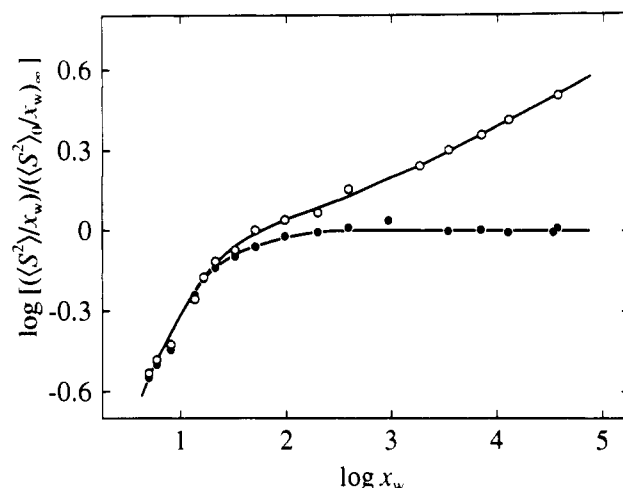


Figure 5. Double-logarithmic plots of $[(\langle S^2 \rangle/x_w)/(\langle S^2 \rangle_0/x_w)]$ against x_w for the a-PS samples ($f_r = 0.59$): (O) in toluene at 15.0 °C; (●) in cyclohexane at 34.5 °C (Θ) (reproduced from refs 17 and 21, except for the sample F380). For the cyclohexane solutions, $\langle S^2 \rangle/x_w$ means $\langle S^2 \rangle_0/x_w$.

Table IV

Values of x_w and α_S^2 for Atactic Oligo- and Polystyrenes in Toluene at 15.0 °C

sample	x_w	α_S^2	sample	x_w	α_S^2
A1000-b	13.7	0.965	F4	384	1.40
A2500-a'	16.6	1.01	F20	1840	(1.75) ^a
A2500-a	21.3	1.03	F40	3450	2.03
A2500-b	32.9	1.06	F80	7040	2.28
A5000-3	51.2	1.15	F128-2	12700	2.65
F1-2	96.6	1.15	F380	36900	3.15
F2	197	1.19			

^a Calculated from eq 2 with $\langle S^2 \rangle_0/x_w = 8.13$ Å².

regarding them as the values for the unperturbed a-PS chain in toluene at 15.0 °C. We may also use the values of the HW model parameters determined from the data for $\langle S^2 \rangle_0$ in cyclohexane at Θ to represent the unperturbed a-PS chain in toluene at 15.0 °C.

For the cyclohexane solutions, the reduced ratio $[(\langle S^2 \rangle_0/x_w)/(\langle S^2 \rangle_0/x_w)_\infty]$ is seen to increase monotonically with increasing x_w and then become unity for $x_w > \text{ca. } 300$. For large x_w , the data points for the toluene solutions deviate upward progressively from those for the cyclohexane solutions with increasing x_w . Clearly this is due to the excluded-volume effect. As x_w is decreased, the effect diminishes, and it completely vanishes for $x_w < \text{ca. } 20$. The critical value of x_w above which the excluded-volume effect on $\langle S^2 \rangle$ becomes appreciable is located around a shoulder of the $\log [(\langle S^2 \rangle_0/x_w)/(\langle S^2 \rangle_0/x_w)_\infty]$ vs $\log x_w$ curve, i.e., in the range of x_w for which the ratio $\langle S^2 \rangle_0/x_w$ has not yet reached its asymptotic value. Recall that this result is consistent with the previous conclusion¹² derived from the simulation of the a-PS chain by the polymethylene-like rotational isomeric state chain with excluded volume (see Figure 1 of ref 12).

Comparison with the Yamakawa-Stockmayer-Shimada Theory. The values of α_S^2 calculated from the defining equation

$$\langle S^2 \rangle = \langle S^2 \rangle_0 \alpha_S^2 \quad (2)$$

with the values of $\langle S^2 \rangle^{1/2}$ and $\langle S^2 \rangle_0^{1/2}$ given in Tables II and III are summarized in Table IV and are double-logarithmically plotted against x_w in Figure 6. Here, the results for the samples OS5, OS6, and OS8 ($\alpha_S^2 = 1.04$ – 1.05) have been omitted to avoid confusion, since α_S must be equal to unity for them. We note that the value of α_S^2

for the sample F20 has been calculated with the value of $\langle S^2 \rangle_0$ estimated from the coil limiting value of $\langle S^2 \rangle_0/x_w$ ($=8.13 \text{ \AA}^2$). It is clearly seen that the excluded-volume effect appears at $x_w = 10$ –20, as mentioned above.

Now we proceed to make a comparison of the present results for α_S^2 with the YSS theory. Thus it is convenient to give a brief description of the theory. For the HW chain of total contour length L , it assumes the Domb-Barrett expression²⁶ for α_S^2 ; i.e.

$$\alpha_S^2 = [1 + 10\bar{z} + (70\pi/9 + 10/3)\bar{z}^2 + 8\pi^{3/2}\bar{z}^3]^{2/15} [0.933 + 0.067 \exp(-0.85\bar{z} - 1.39\bar{z}^2)] \quad (3)$$

with the parameter \bar{z} defined by

$$\bar{z} = (3/4)K(\lambda L)z \quad (4)$$

in place of the excluded-volume parameter z . The latter is defined by

$$z = (3/2\pi)^{3/2}(\lambda B)(\lambda L)^{1/2} \quad (5)$$

where

$$B = \beta/a^2 c_\infty^{3/2} \quad (6)$$

with

$$\begin{aligned} c_\infty &= \lim_{\lambda L \rightarrow \infty} (6\lambda \langle S^2 \rangle_0 / L) \\ &= \frac{4 + (\lambda^{-1}\tau_0)^2}{4 + (\lambda^{-1}\kappa_0)^2 + (\lambda^{-1}\tau_0)^2} \end{aligned} \quad (7)$$

Here, λ^{-1} is the static stiffness parameter of the HW chain, κ_0 and τ_0 are the constant curvature and torsion, respectively, of its characteristic helix taken at the minimum zero of its elastic energy, and β is the binary cluster integral between beads with a their spacing. In eq 4, K is the first-order perturbation coefficient for the mean-square end-to-end distance $\langle R^2 \rangle$, so that

$$\alpha_S^2 = 1 + (67/70)K(\lambda L)z - \dots \quad (8)$$

and it is given by

$$\begin{aligned} K(L) &= \frac{4}{3} - 2.711L^{-1/2} + \frac{7}{6}L^{-1} \quad \text{for } L > 6 \\ &= L^{-1/2} \exp(-6.611L^{-1} + 0.9198 + 0.03516L) \quad \text{for } L \leq 6 \end{aligned} \quad (9)$$

Note that L is related to the degree of polymerization x by the equation

$$L = xM_0/M_L \quad (10)$$

where M_0 is the molecular weight of the repeat unit and M_L is the shift factor as defined as the molecular weight per unit contour length.

Thus α_S^2 is given as a function of L or x and also of the five parameters: $\lambda^{-1}\kappa_0$, $\lambda^{-1}\tau_0$, λ^{-1} , M_L , and the reduced excluded-volume strength λB . When the basic HW model parameters (other than λB) have already been determined, the problem is reduced to a determination of the parameter λB from a best fit of the observed values of α_S^2 to the theoretical values.

The HW model parameters themselves may be determined from a comparison between theory and experiment for $\langle S^2 \rangle_0$, as done previously.¹⁷ Its theoretical expression is given by

$$\langle S^2 \rangle_0 = \lambda^{-2} f_s(\lambda L; \lambda^{-1}\kappa_0, \lambda^{-1}\tau_0) \quad (11)$$

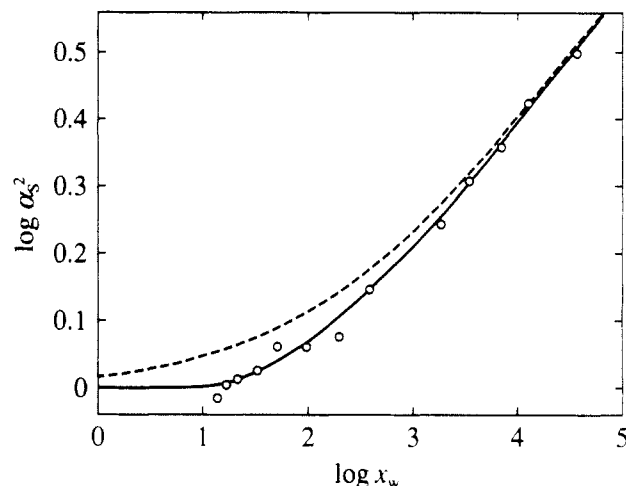


Figure 6. Double-logarithmic plots of α_S^2 against x_w for the a-PS samples ($f_r = 0.59$) in toluene at 15.0 °C. The solid curve represents the best-fit YSS theory values, and the dashed curve represents the conventional two-parameter theory prediction (see the text).

where the function f_s is defined by

$$\begin{aligned} f_s(L; \kappa_0, \tau_0) &= \frac{\tau_0^2}{\nu^2} f_{s,KP}(L) + \frac{\kappa_0^2}{\nu^2} \left[\frac{L}{3r} \cos \varphi - \frac{1}{r^2} \cos(2\varphi) + \right. \\ &\quad \left. \frac{2}{r^3 L} \cos(3\varphi) - \frac{2}{r^4 L^2} \cos(4\varphi) + \frac{2}{r^4 L^2} e^{-2L} \cos(\nu L + 4\varphi) \right] \end{aligned} \quad (12)$$

with

$$\nu = (\kappa_0^2 + \tau_0^2)^{1/2} \quad (13)$$

$$r = (4 + \nu^2)^{1/2} \quad (14)$$

$$\varphi = \cos^{-1}(2/r) \quad (15)$$

and with $f_{s,KP}$ being the function f_s for the KP chain and being given by

$$f_{s,KP}(L) = \frac{L}{6} - \frac{1}{4} + \frac{1}{4L} - \frac{1}{8L^2} (1 - e^{-2L}) \quad (16)$$

Although the values of the HW model parameters for a-PS have already been determined,¹⁷ in this work we redetermine them from an analysis of the data for $\langle S^2 \rangle_0/x_w$ given in Figure 4, since the present asymptotic value of $\langle S^2 \rangle_0/x_w$ for large x_w is somewhat different from the literature value,^{24,25} as stated above. Here, the values of $\lambda^{-1}\kappa_0$ and $\lambda^{-1}\tau_0$ are assumed to be the same as those ($\lambda^{-1}\kappa_0 = 3.0$ and $\lambda^{-1}\tau_0 = 6.0$) determined from $\langle \Gamma^2 \rangle$ as in the previous work.¹⁷ The present results then are $\lambda^{-1} = 20.6 \text{ \AA}$ and $M_L = 35.8 \text{ \AA}^{-1}$. These are somewhat different from the previous estimates ($\lambda^{-1} = 22.5 \text{ \AA}$ and $M_L = 36.7 \text{ \AA}^{-1}$).¹⁷

In Figure 6, the solid curve represents the best-fit YSS theoretical values calculated from eq 3 with these values of the HW model parameters along with $\lambda B = 0.26$. It is seen that there is excellent agreement between theory and experiment in the entire range of x_w studied. For comparison, the two-parameter theory values calculated similarly from eq 3 with $\lambda B = 0.26$ but with $K = 4/3$ (the coil limiting value) are represented by the dashed curve. The latter theory is seen to overestimate α_S greatly for small x_w , in contrast to the experimental results and therefore also to the YSS theory. This is clearly due to neglect of the effect of chain stiffness. In the YSS theory, the effect is taken into account by the coefficient K that decreases extremely rapidly to zero with decreasing L , as

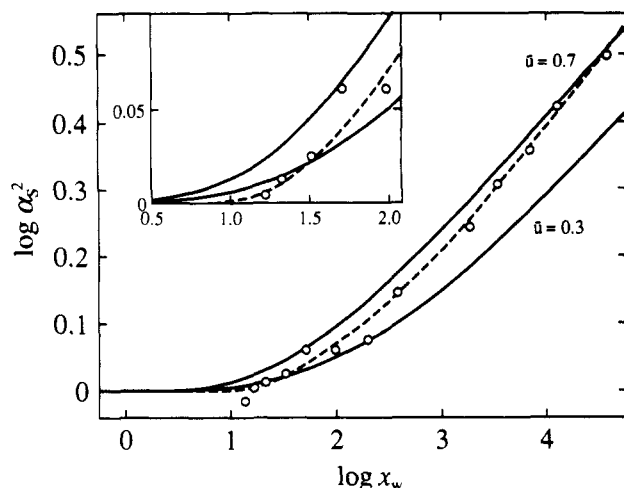


Figure 7. Double-logarithmic plots of α_S^2 against x_w for the a-PS samples ($f_r = 0.59$) in toluene at 15.0 °C. The solid curves represent the Chen-Noolandi theory values with the indicated values of their parameter \bar{u} , and the dashed curve represents the YSS theory values. The inset is an enlargement of the region of small α_S .

Table V
Values of M_w , λL , \bar{z} , and z for Atactic Oligo- and Polystyrenes in Toluene at 15.0 °C

sample	M_w	λL	\bar{z}	z
OS5	5.78×10^2	0.784	4×10^{-5}	0.076
OS6	6.80×10^2	0.922	1×10^{-4}	0.082
OS8	9.04×10^2	1.23	0.001	0.095
A1000-b	1.48×10^3	2.01	0.006	0.122
A2500-a'	1.78×10^3	2.41	0.011	0.133
A2500-a	2.27×10^3	3.08	0.021	0.151
A2500-b	3.48×10^3	4.72	0.047	0.186
A5000-3	5.38×10^3	7.30	0.085	0.232
F1-2	1.01×10^4	13.7	0.163	0.318
F2	2.05×10^4	27.8	0.292	0.452
F4	4.00×10^4	54.2	0.468	0.632
F10	9.73×10^4	132	0.817	0.985
F20	1.91×10^5	259	1.21	1.38
F40	3.59×10^5	487	1.72	1.89
F80	7.32×10^5	993	2.53	2.70
F128-2	1.32×10^6	1790	3.46	3.63
F288-a	3.52×10^6	4770	5.75	5.92
F380	3.84×10^6	5210	6.02	6.19

seen from eq 9. It is also important to see that the effect of chain stiffness (difference between the solid and dashed curves) still remains appreciable even for large $x_w \sim 10^4$ ($M_w \sim 10^6$). Such a slow convergence to the flexible coil behavior arises from the fact that the deviation of K from the coil limiting value $4/3$ varies as $L^{-1/2}$. In this connection, recall that $\langle S^2 \rangle_0/x_w$ is almost independent of x_w for $x_w \gtrsim 300$ ($M_w \gtrsim 3 \times 10^4$).

In order to examine the effect more quantitatively, in Table V are given the values of \bar{z} and z for a-PS in toluene at 15.0 °C calculated from eqs 4 and 5, respectively, with the HW model parameters above along with $\lambda B = 0.26$. It also includes the values of λL calculated from eq 10 with the values of λ^{-1} and M_L above, for convenience. It is seen that \bar{z} is more than 2 orders of magnitude smaller than z for $M_w \leq 10^3$ ($\lambda L \leq 1$). On the other hand, as M_w or λL is increased, the difference between \bar{z} and z becomes smaller, but it still amounts to ca. 7% of \bar{z} at $M_w \approx 10^6$ ($\lambda L \approx 10^3$) and to ca. 3% of \bar{z} even at $M_w = 3.84 \times 10^6$ ($\lambda L = 5.21 \times 10^3$). Strictly, only in the limit of $\lambda L \rightarrow \infty$, \bar{z} becomes equal to z , and then the two-parameter theory for the Gaussian chain becomes valid, so that the original Domb-Barrett equation for α_S^2 (eq 3 with z in place of \bar{z}) holds. For a-PS, such a situation may be realized only in a limited range of extremely high molecular weight, say,

$M_w > 10^7$. Thus we may conclude without much exaggeration that the conventional two-parameter theory is valid only for infinitely high molecular weights. The present conclusion may require reconsideration of the analysis of data for the expansion factor made so far on the basis of the two-parameter theory.

Comparison with the Chen-Noolandi Theory. Very recently, Chen and Noolandi²⁷ have evaluated $\langle R^2 \rangle$, $\langle S^2 \rangle$, and A_2 of the KP wormlike chain with excluded volume by an application of the renormalization group scaling. They have proposed approximate closed interpolation formulas for those quantities as functions of L , the "dimensionless excluded-volume interaction" \bar{u} , and the Kuhn statistical segment length b (in their notation), which is identical with λ^{-1} in the case of the KP chain (HW chain with $\kappa_0 = 0$). In the limits of $L \rightarrow \infty$ and $L \rightarrow 0$, their results reduce to the limiting forms for the Gaussian coil and rigid rod, respectively.

Thus it is interesting to make a comparison of the present experimental values for α_S^2 with the Chen-Noolandi (CN) theory. Figure 7 shows double-logarithmic plots of α_S^2 against x_w . The unfilled circles represent the present experimental values, and the dashed curve represents the same YSS theory values as those in Figure 6. The solid curves represent the CN theory values calculated from eqs 4.2, A6, and A7 of ref 27 with $\bar{u} = 0.3$ and 0.7. Since their α_S^2 is a function of L/b (or λL) if \bar{u} is given, we must assign a proper value to $\lambda^{-1}M_L$ in order to convert λL to x_w by the use of eq 10. As found in the previous study of $[\eta]_0$,²⁰ the values of $\lambda^{-1}M_L$ determined from analyses on the basis of the HW and KP chains are in good agreement with each other, although the individual values of λ^{-1} and M_L are not. Thus we have used the value 738 for $\lambda^{-1}M_L$ obtained from those of λ^{-1} and M_L determined above. The value of 0.7 of \bar{u} has been chosen so that the CN theory values may fit the experimental data in the range of large x_w for which the relation between α_S^2 and z is close to that for the flexible coil. With this value of \bar{u} , the theoretical curve deviates upward progressively from the experimental one with decreasing x_w . On the other hand, the theoretical curve exhibits great deviation at large x_w if it is forced to fit the data points at $x_w \approx 20$ –30 by assuming $\bar{u} = 0.3$. It is clearly seen that the theoretical curves are substantially different from the experimental one in shape. Further, as seen from the inset of Figure 7, the CN theory prediction also yields a marked discrepancy from the experimental observation in the value of x_w for the onset of the excluded-volume effect, irrespective of the value of \bar{u} .

The results predicted by the CN theory are in sharp contrast to those by the YSS theory that explains quite accurately the experimental results. The deficiency of the former may be regarded as arising from the fact that the excluded-volume effect has not been correctly incorporated near the rod limit. Specifically, the ring-closure probability near this limit, the exact evaluation of which is a very difficult step in the theoretical treatment of the problem under consideration, has not been treated at all in the CN theory. In order to make this point more clear, we examine the limiting form of α_S^2 in the limit of $L \rightarrow 0$. In the CN theory, $\langle S^2 \rangle$ of the KP chain with excluded volume is given by eq 16 with $L\mathcal{L}_s$ in place of L , where \mathcal{L}_s is the "rescaled function", i.e., a certain factor to take into account the excluded-volume effect on the chain dimension, so that it becomes equal to unity in the rod limit. If we expand their result for $\langle S^2 \rangle$ in powers of the deviation δ of \mathcal{L}_s from unity and neglect terms of $\mathcal{O}(\delta^n)$ ($n \geq 2$), we have the same expression for α_S^2 as eq 8 but with $K(L)$

given by

$$K(L) = 2.144L^{1/2}[f_{s,KP}(L)]^{-1} \left[\frac{L}{6} - \frac{1}{4L} + \frac{1}{4L^2}(1 - e^{-2L} - Le^{-2L}) \right] \{ [1 + 1.6728f_{s,KP}(L)]^{1/2} - 1 \} \quad (\text{Chen-Noolandi}) \quad (17)$$

In the limit of $L \rightarrow 0$, this $K(L)$ is proportional to $L^{3/2}$, while that given by eq 9 is proportional to $L^{-1/2} \exp(-6.611L^{-1})$. Thus $K(L)$ of the CN theory quite gradually approaches zero compared to that of the YSS theory. This is the reason why the CN theory fails to explain the sudden onset of the excluded-volume effect at $x_w = 10\text{--}20$ (for a-PS).

In sum, it may be said that the CN theory has not essentially treated the excluded-volume effect on $\langle S^2 \rangle$ of a stiff chain. The same remark applies also to their treatments of the excluded-volume effects on $\langle R^2 \rangle$ and A_2 . Their theory is of no practical use, as shown also for other polymers in later papers.

Conclusion

We have determined $\langle S^2 \rangle$ for a-PS in toluene over a wide range of M_w , including the oligomer region. It is found that the results for the radius expansion factor α_S may well be explained by the YSS theory, which takes account of the effect of chain stiffness on the basis of the HW chain. The results show that α_S decreases extremely rapidly to unity with decreasing M_w , as predicted by the theory. The recent renormalization group theory by Chen and Noolandi fails to explain such salient behavior of α_S . The YSS theory also predicts that the effect of chain stiffness on α_S remains rather large even at very large $M_w \sim 10^6$ for a-PS. Despite the fact that the chain stiffness has such significant effects on α_S , it is interesting to conclude that a quasi-two-parameter scheme may be regarded as valid at least for α_S , since there is good agreement between the present experiment and the YSS theory, which assumes that α_S is a function only of the scaled excluded-volume parameter \tilde{z} .

In the following paper,²⁸ we proceed to make a study of another single-chain problem, i.e., the viscosity-radius expansion factor α_η . The interpenetration function Ψ will be studied in a forthcoming paper from the new point of view, as mentioned in the Introduction.

Acknowledgment. This research was supported in part by a Grant-in-Aid (02453100) from the Ministry of Education, Science, and Culture, Japan.

References and Notes

- (1) Flory, P. J. *Principles of Polymer Chemistry*; Cornell University Press: Ithaca, NY, 1953.
- (2) Yamakawa, H. *Modern Theory of Polymer Solutions*; Harper & Row: New York, 1971.
- (3) Freed, K. F. *Renormalization Group Theory of Macromolecules*; Wiley-Interscience: New York, 1987.
- (4) des Cloizeaux, J.; Jannink, G. *Polymers in Solution*; Oxford University Press: Oxford, U.K., 1990.
- (5) Fujita, H. *Polymer Solutions*; Elsevier: Amsterdam, The Netherlands, 1990.
- (6) Huber, K.; Stockmayer, W. H. *Macromolecules* **1987**, *20*, 1400 and also papers cited therein.
- (7) Yamakawa, H. *Macromolecules* **1992**, *25*, 1912.
- (8) Yamakawa, H.; Stockmayer, W. H. *J. Chem. Phys.* **1972**, *57*, 2843.
- (9) Kratky, O.; Porod, G. *Recl. Trav. Chim. Pays-Bas* **1949**, *68*, 1106.
- (10) Yamakawa, H. *Annu. Rev. Phys. Chem.* **1984**, *35*, 23.
- (11) Yamakawa, H. In *Molecular Conformation and Dynamics of Macromolecules in Condensed Systems*; Nagasawa, M., Ed.; Elsevier: Amsterdam, The Netherlands, 1988; p 21.
- (12) Yamakawa, H.; Shimada, J. *J. Chem. Phys.* **1985**, *83*, 2607.
- (13) Shimada, J.; Yamakawa, H. *J. Chem. Phys.* **1986**, *85*, 591.
- (14) Huber, K.; Bantle, S.; Lutz, P.; Burchard, W. *Macromolecules* **1985**, *18*, 1461.
- (15) Kitagawa, T.; Sadanobu, J.; Norisuye, T. *Macromolecules* **1990**, *23*, 602.
- (16) Konishi, T.; Yoshizaki, T.; Shimada, J.; Yamakawa, H. *Macromolecules* **1989**, *22*, 1921 and succeeding papers.
- (17) Konishi, T.; Yoshizaki, T.; Saito, T.; Einaga, Y.; Yamakawa, H. *Macromolecules* **1990**, *23*, 290.
- (18) Orofino, T. A. *J. Chem. Phys.* **1966**, *45*, 4310.
- (19) Bohdanecky, M.; Berek, D. *Makromol. Chem., Rapid Commun.* **1985**, *6*, 275.
- (20) Einaga, Y.; Koyama, H.; Konishi, T.; Yamakawa, H. *Macromolecules* **1989**, *22*, 3419.
- (21) Konishi, T.; Yoshizaki, T.; Yamakawa, H. *Macromolecules* **1991**, *24*, 5614.
- (22) Yamada, T.; Yoshizaki, T.; Yamakawa, H. *Macromolecules* **1992**, *25*, 377.
- (23) Berry, G. C. *J. Chem. Phys.* **1966**, *44*, 4550.
- (24) Miyaki, Y.; Einaga, Y.; Fujita, H. *Macromolecules* **1978**, *11*, 1180.
- (25) Miyaki, Y. Ph.D. Thesis, Osaka University, Osaka, Japan, 1981.
- (26) Domb, C.; Barrett, A. J. *Polymer* **1976**, *17*, 179.
- (27) Chen, Z. Y.; Noolandi, J. *J. Chem. Phys.* **1992**, *96*, 1540.
- (28) Abe, F.; Einaga, Y.; Yamakawa, H. *Macromolecules*, following paper in this issue.